

Contents

1 Belle II and SuperKEKB (SKB) accelerator	3
1.1 Physics program of the B-factories	3
1.1.1 Opened questions in SM	3
1.1.2 Belle II Physics channels	4
1.1.3 B meson decay vertices	6
1.2 SuperKEKB accelerator	8
1.2.1 The facility	8
1.2.2 "Nano-beam" scheme	10
1.3 Belle II detector	11
1.3.1 Vertex Detector (VXD)	12
1.3.2 Central Drift Chamber (CDC)	12
1.3.3 Particle identification system (TOP e ARICH)	12
1.3.4 Electromagnetic calorimeter (ECL)	13
1.3.5 K_L muon detector (KLM)	14
1.3.6 Trigger system	14
1.4 Current state and perspectives of data taking	14
2 Belle II Upgrade	16
2.1 Background sources and limitations in Belle II	16
2.1.1 Major background sources	16
2.1.2 Current background status and future implications (predictions)	17

2.2	Purposes of the upgrade	18
2.3	Summary of possible VXD upgrade	19
2.3.1	DEPFET	19
2.3.2	Thin and Fine-Pitch SVD	20
2.3.3	Silicon On Insulator (SOI)	20
2.3.3.1	Concept	20
2.3.3.2	Sensor design and features	21
2.3.4	CMOS MAPS	23
3	VTX detector	24
3.1	VTX Layout and mechanical structure?	24
3.1.1	iVTX	25
3.1.1.1	R&D	26
3.1.2	oVTX	26
3.1.2.1	R&D	27
3.2	Performance simulation	28
3.3	OBELIX chip design	28
4	Conclusions	30

1. Belle II and SuperKEKB (SKB) accelerator

This first chapter aims to present a brief introduction of the Belle II physics program, focusing on those measurements which could particularly benefit from the upgrade of the whole detector and especially of the VerteX Detector (VXD). A short description of the SuperKEKB accelerator and the Belle II detector's structure are also presented and to conclude some highlights on the actual state of measurements.

1.1 Physics program of the B-factories

Belle II is a B-factory dedicated to improve precision measurements of the Standard Model's parameters (SM) and to looking for the physics Beyond the Standard Model. In particular the experiment investigates the Charge-Parity Violation (CPV) in the B mesons system and it also searches for new physics evidences in the decays of B and D mesons, in τ leptons and in the dark matter sector (DM), above all, hunting for dark photons.

1.1.1 Opened questions in SM

The SM is a physics theory that describe three of the fundamental forces involving elementary particles, which are strong, weak and electromagnetic interaction (with the exclusion of the gravitational one). It classifies all particles known so far, in 4 main groups: quark, leptons, bosons and Higgs (figure 1.1 on the following page).

Despite its undeniable success in predicting with high precision new particles and unknown mechanisms over the years, there are many aspects of the Nature on which it is unable to give answers. Some of them are listed in the following.

- Three generations of quark and leptons are known, but it is not obvious whether they should be the only ones and the reasons behind their mass hierarchy.
- Higgs mechanism is able to explain the cause of elementary particles' masses through spontaneous electro-weak symmetry breaking, but it doesn't justify those of neutrinos.
- The SM also predicts other Higgs-like bosons, potentially vector bosons, whose existence would be justified in some SUper-SYmmetry (SUSY) theories or in others of New Physics.



Figure 1.1: Particle classification in the Standard Model.

- Another opened question is the matter-antimatter asymmetry in the Universe. Even though CP violation is necessary to explain the current state of the universe, the observed quantity is several orders of magnitude less than needed to explain the matter domination over antimatter, which allowed the evolution of the universe as we know it today.
- In the SM the Cabibbo-Kobayashi-Maskawa (CKM) matrix describes the flavour-changing weak interaction through the mismatch between the quantum state of the freely propagating quarks. It could be parametrized by three mixing angles and a complex phase that is at the foundation of CP Violation in the quark flavor sector. The fact that its elements are almost diagonal might suggest the existance of a new symmetry, that is unbroken at high energy (greater than the order of TeV).

All these topics encourage the research of new particles and processes that could give reasonable answers.

At the energy frontier, experiments like the Large Hadron Collider (LHC) in Geneve are looking for new particles created from the proton-proton collision with a center mass energy up to 14 TeV.

At luminosity frontier instead, the trace of new particles and mechanisms is searched in precision measurements of suppressed reactions in flavour physics or in the deviations from SM. The discrepancies indeed, could be interpreted as a clue of new physics beyond SM. The last is the Belle II approach.

1.1.2 Belle II Physics channels

SuperKEKB has a very broad field of research and in the following we will go through the main physics goals of the experiment, underlining how the measurements could be enhanced by the upgrade of the vertex detector.

FLAVOR PHYSICS

CP-violating phases in quark sector:

- as we mentioned above, the amount of CP violation in the SM is not enough to explain the difference observed between baryon-antibaryon matter. New clues of CPV could be found studying the discrepancy between B^0 and \bar{B}_0 decay rates, so measuring the time-dependent CP violation in penguin transition of $b \rightarrow s$ and $b \rightarrow d$ quarks (such as $B \rightarrow \phi K^0$ and $B \rightarrow \eta' K^0$). In fact this violation is predicted to be very small and so any significant observation can be interpreted as a signal beyond the SM.
- Also the CP violation in charm mixing, negligible in the SM, could draw attention to new phenomena in the up-type quark sector (up, charm, top).
- Another aspect that need to be understood is the large amount of CP violation in the time-integrated rates of charmless hadronic B decays, such as $B \rightarrow K\pi$ and $B \rightarrow K\pi\pi$, observed by LHCb and other B factories.

Conclusive measurements of time-dependent CP violation require a combination of data size and high precision measurement of Δz (discussed further in section "B meson decay vertices" on the next page), such as the distance between the tag and the signal in B meson decay vertices. In this respect, the upgrade of VXD could improve a lot the flavor tagging efficiency losses, due mainly to the beam-induced backgrounds, among others reasons.

Multiple Higgs bosons: Another relevant measurement is the Branching Ratio (BR) of the channel $B \rightarrow \tau\nu$, which is particularly sensitive to the charged Higgs boson (in addition to a neutral SM-like Higgs) that in general couples more strongly to heavier particles. Likewise the BR of the decay $B \rightarrow D^{(*)}\tau\nu$, where BaBar, Belle and LHCb had already reported some anomalies. Extended Higgs mechanism could introduce extra sources of CP violation that we are looking for.

We could notice that semi-tauonic decay measurements like these, rely on efficient and full reconstruction of B mesons and so on the performance of VXD.

Flavor Changing Neutral Current (FCNC):

- The leading measurements suitable for this purpose are the time-dependent CP violation in $B \rightarrow K^{*0}(\rightarrow K_S^0 \pi^0)\gamma$, triple product CP violation asymmetries in $B \rightarrow VV$ decays, and semileptonic decays $B \rightarrow Vl\nu$, $V = D^*, \rho$.
- It is also essential to measure $b \rightarrow s\nu\bar{\nu}$ transitions (such as $B \rightarrow K^{(*)}\nu\bar{\nu}$) which belong to a class of decays with large missing energy and also improve FCNC measurements of $b \rightarrow d$, $b \rightarrow s$, and $c \rightarrow u$ transitions.

Most of the analyses with missing energy in the final state utilise hadronic or semileptonic B full reconstruction techniques and the success of these methods is mostly dependent on low momentum track finding and so on the capabilities of the vertex detector as well.

Sources of Lepton Flavor Violation (LFV): LFV in charged lepton decay is a key prediction in many neutrino mass generation mechanisms and other models of physics beyond the SM. Belle II has an unrivalled sensitivity to τ decays, because of their production in a clean e^+e^- collision background and the large dataset available. The experiment analyzes τ leptons to search for LF and CP violation and to measure its electric dipole moment and $(g-2)$ value.

NON FLAVOR PHYSICS

Dark Sector: Belle II has a unique sensitivity to dark matter via missing energy decays. Although most researches for new physics are indirect, there are different models that predict the existence of new particles at the mass scale from MeV to TeV, that couple to the SM via new gauge asymmetries. They also predict a vast range of hidden particles, including dark matter candidates and new gauge bosons.

In these last two areas, τ and dark sectors physics, the aim is to probe forbidden and ultra-rare transitions in low-multiplicity final states with as large dataset as possible. This mostly relies on trigger efficiency and strategies, that could take advantage from the upgrade. Many of these processes can only be addressed by Belle II, so it is essential to increase the performance of the detector.

Binding Hadrons: As time goes on, a large number of states not predicted by conventional mesons interpretation are discovered in other B factories and hadron colliders, changing our understanding of QCD in the low-energy regime. For this reason, study of quarkonia is a fundamental purpose for Belle II. In fact new particles can be produced near resonance, achievable by adjusting the machine energy or by initial state radiation, which effectively provides a continuum of center of mass energies.

CKM matrix: Belle II is also dealing with the measurements of CKM observable, the matrix elements and their phases, with unprecedented precision.

1.1.3 B meson decay vertices

The main task of VXD is to reconstruct the production and decay vertices of the particles originated from the beam collisions. This aspect is crucial to perform time-dependent measurements, core of the Belle II physics program, that we have briefly introduced in the previous.

The center of mass energy of Belle II experiment has its peak at the $\Upsilon(4S)$ resonance, such as $\sqrt{s} = 10.58$ GeV, which decays almost instantaneously into two B mesons ($B^0 \bar{B}^0$) in nearly 96% of all cases. The choice of the asymmetric configuration of the beams relies precisely in the requirement to boost the

mesons in order to measure their life-time, exploiting the information on the distance between their decay vertices. In fact in a beam symmetric situation, they would have been produced at rest, decaying roughly at the same point or in any case at undetectable distances. The investigation of CP Violating processes instead, requires to measure the decay time difference of the two B mesons, and its uncertainty is dominated by that of decay vertex measurement (order of hundreds microns). Let us look at this in more details.

SuperKEKB collides an electrons beam of 7 GeV with a positrons beam of 4 GeV, chosen in order to have the center mass energy equal to 10.58 GeV. Indeed it must be valid:

$$s = (p_{e^-}^\mu + p_{e^+}^\mu)^2 = m_{\Upsilon(4S)}^2, \quad \text{with } m_{e^{+/-}} \ll E_{e^{+/-}} \quad (1.1)$$

$$\Rightarrow 4E_{e^-} - E_{e^+} = m_{\Upsilon(4S)}^2 \quad (1.2)$$

So it's possible to compute the Lorentz boost of the mass center:

$$\vec{P}_{\Upsilon(4S)} = \vec{p}_{e^-} + \vec{p}_{e^+} = (\beta\gamma)_{\Upsilon(4S)} m_{\Upsilon(4S)} \approx 3 \text{ GeV} \quad (1.3)$$

$$\Rightarrow (\beta\gamma)_{\Upsilon(4S)} = \frac{3 \text{ GeV}}{10.58 \text{ GeV}} \approx 0.28 \quad (1.4)$$

which is the same boost acquired by mesons, because they are produced almost at rest ($m_{\Upsilon(4S)} - m_{B_0} \approx 19 \text{ MeV}$). Moreover knowing that $\tau_B \simeq 1.5 \times 10^{-12} \text{ s}$ and so $c\tau_B \simeq 450 \mu\text{m}$, we can compute the average flight distance travelled before decaying:

$$l = (\beta\gamma)_{\Upsilon(4S)} c\tau_B \approx 126 \mu\text{m} \quad (1.5)$$

This value must be within the vertex detector sensitivity in order to distinguish the vertex decay and as consequence a precision measurements of lifetimes, mixing parameters and CP violation. The six-layer VXD could determine the position of the vertices with a precision better than $100 \mu\text{m}$, allowing to reconstruct secondary vertices, i.e. the decay position of the particles coming from B decays, and also the tau and D mesons vertices. [In the topology of the B meson decay vertices, lie the combined great efforts employed to be able to build a fast, high-granularity and radiation hardness detector]

Now let us take a closer look at the event kinematics (e.g. figure on the following page). The two B mesons are produced in an entangled quantum state, so from the decay products of the first it's possible to assign its flavor (for example B^0 , identified as B_{tag}^0) and as consequence that of the second, which will be the opposite (\bar{B}^0 , called \bar{B}_{phys}^0).

After this reconstruction, both B decay vertex positions z_1 and z_2 are evaluated, in order to compute their difference:

$$\Delta z = z_1 - z_2 = (\beta\gamma)_{\Upsilon(4S)} c\Delta t \quad (1.6)$$

where Δt is the proper time decay difference. Therefore this topology allows to transform a temporal information in a spatial one that we are able to measure. Without the boosted center of mass none of it could be possible, and this is a

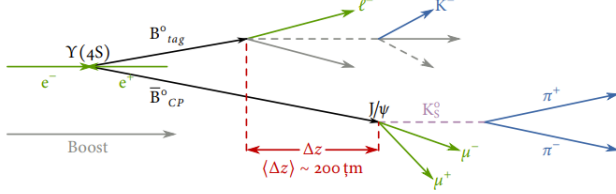


Figure 1.2: Example of the kinematics of the golden channel of Belle II experiment.

main feature for an asymmetric B-factory.

1.2 SuperKEKB accelerator

Belle II sensitivity in the precision measurements that we sift through in the previous section, is feasible especially thanks to the extraordinary performance of the SuperKEKB accelerator which host the (almost) hermetic detector. This complex facility is the result of efforts and efficient collaboration between the researchers of KEK laboratory and all the international working groups that participate to the experiment.

1.2.1 The facility

SuperKEKB is an asymmetric e^+e^- collider with a circumference of 3 km and a center of mass energy peak equal to $\sqrt{s} = 10.58$ GeV, which corresponds to the mass of the $\Upsilon(4S)$ resonance. Compared to its predecessor KEKB (which started its operation in 1998 and concluded in 2010), the current accelerator has allowed to obtain the highest luminosity ever achieved, equal to 4.7×10^{-34} $cm^{-2}s^{-1}$ in July 2022. It was possible only by using a new scheme to accelerate and collide the beams, the so called *nano-beam scheme* (section 1.2.2 on page 10). Moreover a new upgrade of the machine, still under study, will also include other interventions especially to cope with higher background levels, in view of further increase in luminosity.

We will briefly see the main features and parameters of the accelerator.

Luminosity

Instantaneous luminosity is one of the key parameters of any accelerator and it represents the interaction rate per unit of cross section between colliding particles. Reversing this equation is possible to obtain N, namely the number of the physical events produced in the interaction with a given luminosity:

$$L = \frac{1}{\sigma} \frac{dN}{dt} \quad \Rightarrow \quad N = \int_0^T L \sigma dt \quad (1.7)$$

where T is the duration of the experiment, σ the cross section of the physical process of interest. Specifically luminosity is strictly dependent from both machine and beam parameters. With respect to this, it can be expressed as:

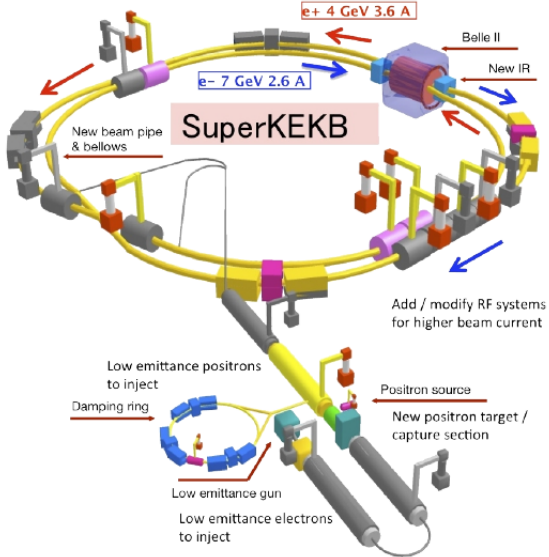


Figure 1.3: SuperKEKB accelerator structure.

$$L = \frac{\gamma_{\pm}}{2er_e} \left(1 + \frac{\sigma_y^*}{\sigma_x^*}\right) \left(\frac{I_{\pm}\xi_{y\pm}}{\beta_y^*}\right) \left(\frac{R_L}{R_{\xi_{y\pm}}}\right) \quad (1.8)$$

where "±" denotes respectively positrons and electrons, $\sigma_{x,y}^*$ is the beam size at the IP in the horizontal and vertical plane, I is the beam current, β_y^* the vertical beta function at the IP. $\xi_{y\pm}$ is the vertical beam parameter which include the horizontal beta function at the IP, the horizontal emittance, the bunch lenght and the crossing angle between the beams. R_L and $R_{\xi_{y\pm}}$ are the reduction factors due to geometrical loss such as the hourglass effect and finite crossing.

As we have already seen, SuperKEKB holds the actual world record in luminosity (with $\beta_y^* = 1.0$ mm) and in the near future the target will be to reach $6.3 \times 10^{-35} \text{ cm}^{-2}\text{s}^{-1}$ (by 2030), by increasing current beams and reducing their section in the Interaction Point (IP), through the reduction of the betatron function to $\beta_y^* = 0.3$ mm. But this process makes the beam-induced background grow a lot, risking deterioration and not well-functioning of the detectors.

For these reasons, the supervision of the beams background becomes crucial: right now it has been estimated that the background should remain acceptable up to a luminosity value equal to $2.8 \times 10^{-35} \text{ cm}^{-2}\text{s}^{-1}$ with $\beta_y^* = 0.6$ mm. So the chance to achieve higher luminosity is closely related to an upgrade plan of both the detector and the accelerator.

Beam energy

Energy beams is mostly decided by the physics program interesting for the experiment. Currently SuperKEKB collides an electron beam with energy of 7

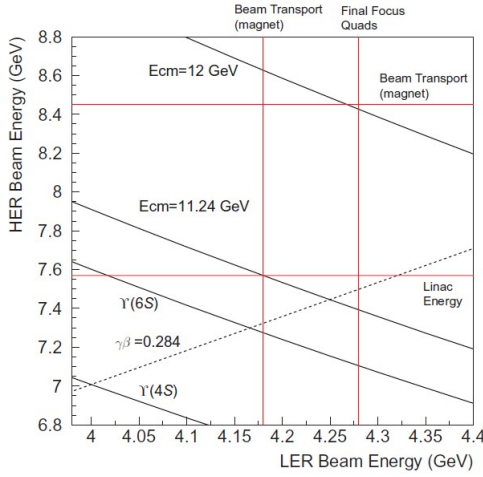


Figure 1.4: Beam energies to reach center of mass energy equal to $\Upsilon(4S)$, $\Upsilon(6S)$, 11.24 GeV and 12 GeV. Horizontal axis represents the energy of LER and the vertical one the energy of HER.

GeV (High Energy Ring, HER), with a positron beam of 4 GeV (Low Energy Ring, LER), reaching a center of mass energy peaked to $\Upsilon(4S)$ resonance.

The choice of colliding asymmetric beam (like its predecessor KEKB, which got collide electrons beam of 8 GeV with a positrons beam of 3.5 GeV) is necessary to identify and measure the decay vertices of particles created in the collisions, as we have seen in section 1.1.3 on page 6.

Indeed this mechanism allows to boost the decay products, improving the vertices reconstruction and increasing the sensitivity of the physics measurement, too.

In figure 1.4 the flexibility of the energy of both LER and HER beams is showed, which provides a continuum of the center mass energy. The possible range covers energies which goes from the $\Upsilon(1S)$ (9.46 GeV) resonance to the $\Upsilon(6S)$ (11.24 GeV).

1.2.2 "Nano-beam" scheme

As mentioned in the previous section, another decisive factor to define the luminosity is the *beta function* β in the Interaction Point (IP). To be able to increase luminosity, it's necessary to decrease the value of β depending also but not only, on the variation of the other machine parameters in the definition (1.8 on the preceding page). The mechanism used in SuperKEKB is called *nano-beam scheme*, and it allowed to obtain luminosity 40 times greater than that of KEKB, managing to decrease of 1/20 the β function in the IP.

This new scheme, designed by P. Raimondi, dictates that the beams have to collide at large angle, equal to 83 mrad in SuperKEKB (keeping beams divided through quadrupole magnets), in order to reduce the *hourglass effect*, which succeed when the bunches in the beam are much longer.

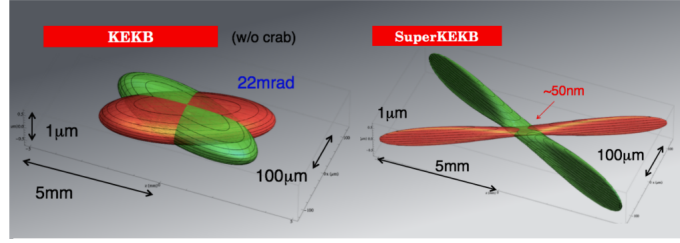


Figure 1.5: Comparison between the beams scheme used in KEKB and SuperKEKB.

Using a crossing angle large enough, has other positive implications on the operation of the accelerator:

- allows the placement of a new focusing system in the IP with a superconducting quadrupole magnet;
- allows to have two distinct line which host HER and LER beams;
- diminishes the *fringe fields* effect in the IP, which are the residuals of the magnets (magnetic fields) in the nearby.

1.3 Belle II detector

Belle II detector is a general-purpose spectrometers, which consists of a series of nested subdetectors placed around the berillium beam pipe of 10 mm of radius, at the IP of the two beams. Here we will go through a brief description of the several subdetectors.

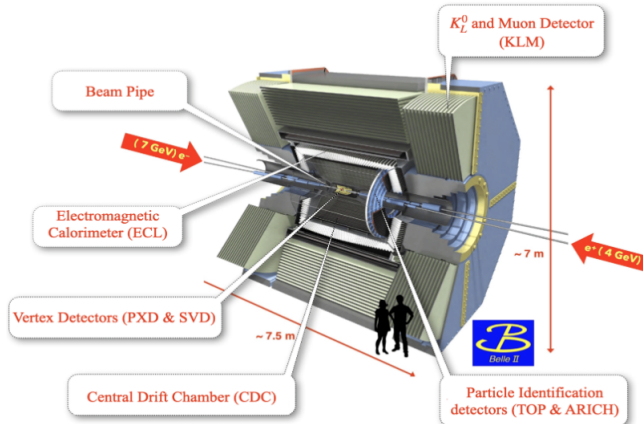


Figure 1.6: Belle II detector.

1.3.1 Vertex Detector (VXD)

The **VerteX Detector (VXD)** is composed by two devices, the silicon Pixel Detector (PXD) and the Silicon Vertex Detector (SVD), for a total of six layers around the beam pipe.

The inner two layers of PXD (L12) consist of pixelated sensors based on the depleted field effect transistor (DEPFET) technology, realised with very thin ($< 100 \mu\text{m}$) sensors, allowing to minimise multiple scattering, thus improving the tracking resolution for low-momentum particles. They are at a radius of 14 mm and 22 mm, respectively.

The remaining four layers of SVD (L3456) instead, are equipped with double-sided silicon strip (DSSD) sensors (at 39 mm, 80 mm, 104 mm and 135 mm respectively). Since a lower background rate is expected with respect to PXD, DSSD allow to achieve similar performance with a much smaller number of readout channels. These layers are mainly used for tracking/vertexing and also for particle identification (dE/dx).

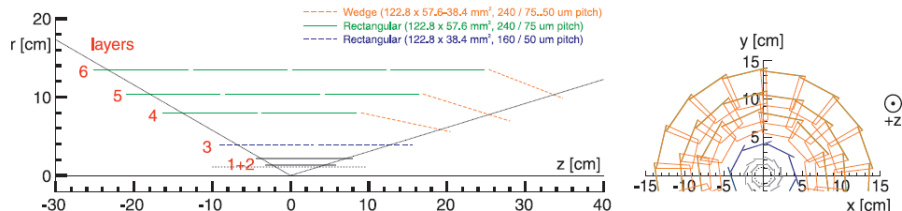


Figure 1.7: A schematic view of the Belle II vertex detector with a Be beam pipe and the six layers of PXD and SVD.

1.3.2 Central Drift Chamber (CDC)

It is the central tracking device, with a large-volume drift chamber and small drift cells. The chamber gas is composed of a He–C₂H₆ 50:50 mixture with an average drift velocity of $3.3 \mu\text{s}^{-1}$ and a maximum drift time of about 350 ns for a 17 mm cell size. The CDC contains 14336 wires arranged in 56 layers either in *axial* (so aligned with the solenoidal magnetic field) or *stereo* (skewed with respect to the axial wires) orientation. In fact by combining information from both the axial and the stereo layers it is possible to reconstruct a full three-dimensional helix charged tracks and measure their momenta. It also provides information for particle identification by measuring ionization energy loss, which is particularly useful for low-momentum particles that cannot reach the outer particle identification subdetectors.

1.3.3 Particle identification system (TOP e ARICH)

TOP (Time Of Propagation) is a special kind of Cherenkov detector used for particle identification in the barrel region. It employs the two-dimensional information of a Cherenkov ring image, such as the time of arrival and the impact position of Cherenkov photons at the photodetector at one end of a 2.6 m quartz bar. It is composed by 16 detector modules, each one consisted in

a 45×2 cm quartz bar (Cherenkov radiator) with a small expansion volume (about 10 cm long) at the sensor end of the bar. In order to achieve a single-photon time resolution of about 100 ps (required for a good PID), 16-channel microchannel plate photomultiplier tubes (MCP-PMT), specially developed for this purpose, are employed.

This detector is the one that creates the greatest concern for higher values of background. [?]

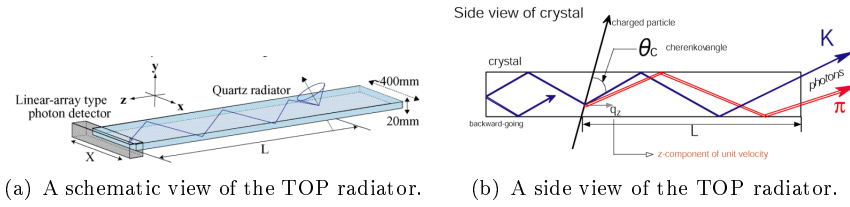


Figure 1.8: TOP detector.

ARICH (Aerogel Ring Imaging CHerenkov) is used to identify charged particle and it is placed in the forward endcap region. It is a proximity focusing Cherenkov ring imagine detector which adopts aerogel as Cherenkov radiator. In particular this detector employs a novel method to increase the number of detected Cherenkov photons: two 2 cm-thick layers of aerogel with different refractive indices ($n_1 = 1.045$ upstream, $n_2 = 1.055$ downstream) that increase the yield without degrading the Cherenkov angle resolution. A hybrid avalanche photon detector (HAPD) are exploited as single-photon-sensitive high-granularity sensor. Here photo-electrons are accelerated over a potential difference of about 8 KV and are detected in avalanche photodiodes (APD).

The main task of these detector is to improve the K/π separation until 3.5 and 4 GeV/c of momentum, respectively.

1.3.4 Electromagnetic calorimeter (ECL)

The **ECL** is a highly segmented array of tellium-doped caesium iodide CsI(Tl) crystals assembled in a 3 m long barrel section with a radius of 1.25m, and two endcaps discs located at 2 m (forward) and 1 m (backward). All of them are instrumented with a total of 8736 crystal, covering about 90 % of the solid angle

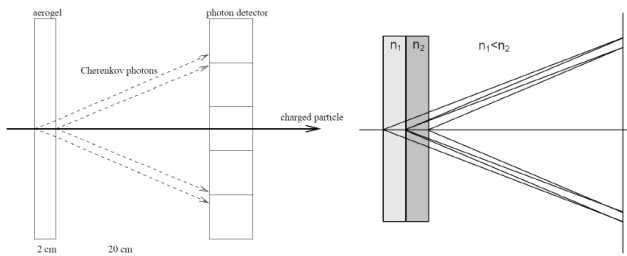


Figure 1.9: ARICH detector.

in center-of-mass system. This detector is used to detect gamma rays and to identify electrons in order to separate the latter from hadrons, especially pions.

1.3.5 K_L muon detector (KLM)

It consists of an alternating sandwich of 4.7 cm-thick iron plates and active detector elements located outside the volume of the superconducting solenoid that provides a 1.5 T magnetic field. The iron plates serve as the magnetic flux return joke for the solenoid. They also provide 3.9 interaction lengths or more of material, beyond the 0.8 interaction lengths of the calorimeter, in which K_L^0 mesons can shower hadronically. The active detector elements have been chosen in order to cope with the reduction of the detector efficiency under the SuperKEKB background rates: resistive plate chambers (RPCs) for the outermost active layers, and scintillator strip with wavelength-shifting fibers, readout by silicon photomultipliers (SiPMs), in the two innermost layers of the barrel and endcaps regions.

1.3.6 Trigger system

The trigger system of Belle II has a non-trivial role to identify events of interest during data-taking at SuperKEKB, where high background rate are expected. This system is composed of two levels: a hardware-based low-level trigger (L1) and a software-based high-level trigger (HLT), implemented in the data acquisition (DAQ) system.

- **L1:** has a latency of 5 μs and a maximum trigger output rate of 30 kHz, limited by the read-in rate of the DAQ.
- **HLT:** is a key component of the DAQ, used to fully reconstruct events that passed the L1 trigger selection. It has to reduce online event rates to 10 kHz for offline storage and it must identify track regions of interest for PXD readout in order to reduce data flux. It fully recreates events with offline reconstruction algorithms, using all detectors information except for the PXD.

1.4 Current state and perspectives of data taking

As we already said, Belle II has reached the world record luminosity with $L_{MAX} = 0.47 \times 10^{-35} \text{ cm}^{-2}\text{s}^{-1}$ in June 2022. In further perspectives, the target is to achieve a new record with $L = 6 \times 10^{-35} \text{ cm}^{-2}\text{s}^{-1}$ and to increase the integrated luminosity from 428 fb^{-1} (actual value, starting in 2019) to 50 fb^{-1} , in order to increase the statistics and also the hope to give an insight in some of the opened questions in the SM.

In order to accomplish the fixed goals mentioned above, an upgrade not only of the vertex detector but of the whole experiment is necessary, among several reasons, to cope with a more complex circumstances due to the increased luminosity, which undermine its proper functioning.

Therefore a three-phase program has been drawn up:

- **short term:** year 2022. Long Shutdown 1 (LS1) is planned for approximately 15 months starting in July 2022, to install a complete pixel detector (PXD). Was it done?
- **short term:** approximately year 2026-27. Long Shutdown 2 (LS2) will probably be needed for the upgrade of the Interaction Region (IR) to reach a new luminosity target $L_{peak} = 6.5 \times 10^{-35} \text{ cm}^{-2}\text{s}^{-1}$. A new Vertex Detector might be required to accommodate the new IR design, and other sub-detector upgrades are possible.
- **long term:** years > 2032 . Studies have started to explore upgrades beyond the currently planned program, such as beam polarization and ultra-high luminosity, such as L_{peak} in excess of $1 \times 10^{-36} \text{ cm}^{-2}\text{s}^{-1}$. While the beam polarization has a concrete proposal, for ultra-high luminosity studies have just started.

At time of writing we are in the period of a long shut-down (LS1), last since June 2022 and the restart of data taking is planned at the beginning of 2024.

2. Belle II Upgrade

This second chapter wants to address some of the main reasons in favor of the upgrade of Belle II. We will give an overview of the primary background sources in the experiment to understand how to mitigate them to be able to achieve a better performance of the whole detector, even ramping up the luminosity. Eventually we will also introduce some of the proposals made for the vertex detector, which is the focus of this thesis.

2.1 Background sources and limitations in Belle II

SuperKEKB is already the world's highest-luminosity collider and it aims to reach a new luminosity peak and to increase the statistics in the future, to become more sensitive to rare processes and precise measurements of Belle II physics program. But to be able to do this without losing the good functionality of the entire detector, it's necessary to understand how to reduce the beam background where possible and how to cope with the consequent challenges.

Several simulations and measurements of beam background are still being done in order to guess possible future machine scenarios, under new luminosity conditions. This is necessary to study the vulnerability of the subdetectors (and more generally of the machine) and so to design the countermeasures to adopt against the deterioration of performance and material.

2.1.1 Major background sources

Making clear that even the interaction of the beams is a source of noise for the measurements, in the following are listed some of the *beam-induced* and *luminosity-dependent* background sources.

Touschek effect : It is an intra-bunches scattering process, where the Coulomb scattering of two particles in the same beam bunch causes a variation of their energies, increasing the value of one of them and lowering that of the other from the nominal value. This interaction among the bunch particles is the first beam background source at SuperKEKB.

Beam-gas scattering : this represents the collision of beam particles with residual gas molecules in the beam pipe. It's the second beam background source and it can occur via two processes: Coulomb interactions, which changes the direction of the beam particles, and bremsstrahlung scattering, which instead decreases their energy.

Because of these two processes, the scattered particle fall out the stable orbit and hit the beam pipe while they move around the ring. This causes electromagnetic showers that could reach the detector if their origin (loss position) is close to it.

Radiative Bhabha scattering and two-photon processes : There are several undesirable collision processes at IP, which have very high cross sections but only little interest for the physics studied in the experiment. Two of them are **Bhabha scattering** ($e^+e^- \rightarrow e^+e^-\lambda$) and **two-photon processes** ($e^+e^- \rightarrow e^+e^-e^+e^-$). In the first channel the emitted photon interacts with the iron magnets and produces a very large amounts of neutrons via the photo-nuclear resonance mechanism. [Such neutrons are the main background source for the outermost Belle II detector, the K_L and muon detector (KLM).] The electrons-positrons pairs of the latter instead, can spiral around the solenoid field lines and leave multiple hits in the inner layers of the detector.

These processes increase the Belle II occupancy and radiation dose, and they are referred as *Luminosity background* because their strength is proportional to the luminosity. The future upgrade intends to deal with this problem in order to keep occupancy low.

Synchrotron Radiation (SR) : X-rays emitted from the beam when electrons and positrons pass through the strong magnetic field near the IP. The HER beam is the main source of this type of background, because SR power is proportional to the square of beam energy and magnetic field. SR can potentially damage the inner layers of the vertex detector due to an higher radiation dose. As a matter of fact, many current studies aim to enhance radiation hardness detector.

There are also other background sources beyond those mentioned above and during the last decade a well-structured set of countermeasures have been developed trying to ease each one of them.

2.1.2 Current background status and future implications (predictions)

Several monitoring devices are located all along the accelerator to keep under control radiation doses on both detector and delicate regions of the ring, to intervene as soon as possible in case too high levels are reached. Indeed large doses of radiation could cause accidental damages on the detector, decreasing its performance.

Event though the current level is of no concern in terms of occupancy for the innermost layers of the vertex detector, in the case of a larger amount of SR, for example, it may cause inhomogenities in PXD module, which would make more difficult to compensate them by adjusting the operation voltages of the affected ones.

Until now it can be said that SuperKEKB and Belle II are operating stably. Beam-induced background rates are well below the limits of the detector and do not prevent from increasing further the current and hence the luminosity.

Despite that, there are several other difficulties that can limit beam currents and so the possibility to move the luminosity frontier at towards higher levels, allowing Belle II reaserchers to study rare physics processes.

2.2 Purposes of the upgrade

Current studies foresee that SuperKEKB may reach higher luminosity targets with the existing accelerator complex (background simulations have been done for each phase listed in section on page 14), but in order to achieve the established final value of $6.3 \times 10^{-35} \text{ cm}^{-2}\text{s}^{-1}$ by 2030, an enhancement of the interaction region are under consideration.

Belle II detector is also designed to operate efficiently under the high levels of backgrounds extrapolated to luminosity target, but safety margins are not so large. Moreover in the case of a redesign of the interaction region large uncertainties in the background extrapolations are unavoidable.

Therefore the global upgrade program is justified by many considerations, among them:

- improve detector's resistance to higher level of background;
- make each subdetectors long-lived against radiation damage;
- push forward safety margins for running at higher luminosity;
- develop the technology to cope with different future paths;
- improve overall physics performance.

In particular all different upgrade ideas of the whole Belle II detector intend to ensure its proper functioning, at the higher level of luminosity ever achived, condering also further improvements of the lattice machine and so of the colliding beams. Indeed current detector configuration is not expected to maintain its performance level when facing high beam background level or high rates.

In regards to the Vertex Detector, all proposed improvements aim to:

- reduce occupancy level by employing fully pixelated and fast detector (nowadays CMOS technologies are the most probably choice);
- increase robustness against tracking efficiency and resolution losses from beam background;
- improve radiation hardness for delaying detector ageing effects and so performance degradation;
- reduce the inserted material budget between subdetectors in order to achieve good resolution lessening the multiple scattering, above all at lower momenta.

2.3 Summary of possible VXD upgrade

The Vertex Detector is particularly sensitive to machine background, being the closest to the beam pipe and therefore subject to high doses of radiation. As we have already seen, current studies are trying to extrapolate how it could be affected by reaching the future luminosity target, but there are a lot of uncertainties due to models and still not well defined design of the interaction region. Moreover a completely new detector might be required, in event of a considerable(significant) redesign of the IR. However in this case, also the physics performance could be improved, taking advantage of the more recent technology developments.

In the following we will present in a few words the four main proposal for future upgrade: DEPFET pixel, thin sensor, CMOS MAPS pixel and SOI technology. The first two are more conservative and try to exploit as much as possible of the existing detector, making some appropriate adjustments (where necessary?) to the sensor type, readout or mechanical structure. The last ones instead, plan to build an entirely new detector.

During the design of all of them, some reference radiation levels have been considered to ensure that the innermost layers background robustness of the upgraded detector was suitable:

- Hit rate capability: $120 \text{ MHz}/\text{cm}^2$;
- Total Ionizing Dose: 10 Mrad/year ;
- NIEL fluence: $5 \times 10^{13} n_{eq}/\text{cm}^2/\text{year}$.

2.3.1 DEPFET

This first proposal intend to minimize risk and costs of the project, preserving the general layout of the PXD system. The upgrade consists to improve the sensor above all, in order to provide higher safety factor for the allowed occupancy and to prevent some issue that at the moment weaken the good functionality of the detector.

Some of the main improvements are listed below:

- improve signal transmission on the pixel matrix and the signal processing in the read-out, in order to reduce the read-out time per row from the current 100 ns to 50 ns. In this way the frame time and the background occupancy might be reduced by factor 2, while leaving unchanged the optimized pixel size and number of PXD as it stands;
- increase the robustness against beam losses which could make inefficient or even inoperative gate lines on almost all PXD modules. This reaction seems to be due to a high photocurrent on the chip because of the high instantaneous dose. It could be mitigate by adding protection circuits on-chip;
- TID effect on the chip provokes an unexpected avalanche current that does not compromise the sensor performance but requires more power supply

to provide enough current. This issue might be solved by bringing some changes in the DEPFET pixel layout.

Simulations and studies of the new pixel design are showing promising results.???

2.3.2 Thin and Fine-Pitch SVD

The Thin and Fine-Pitch SVD (**TFP-SVD**) is a new detector concept that aims to improve not only SVD, but also the inner part of the CDC, whose functionality could be threatened by future beam background condition. This proposal takes into account the Double-sided Silicon Strip Detector (DSSD) as a prime candidate for a tracking device in the inner and middle detector volume since a single sensor can cover a large dimension of about $100 \times 100 \text{ mm}^2$. In the current detector, the DSSD technology is already used in the SVD, which deals with vertex reconstruction and low momentum tracking, together with PXD.

One of the major improvements of this technology is the reduction of the material budget. Currently SVD has about $0.7\%X_0$ material budget per layer. TFP-SVD instead, decreasing the sensor thickness to $140 \mu\text{m}$, intend to reduce it to $0.41\%X_0$.

Moreover small sensor thickness is expected to reduce the voltage needed to reach the full depletion, even after radiation damage. SNAP128 is the front-end thought for TFP-SVD, with 128 input channels and a 127 MHz clock in each of them, to generate the binary hit information sampled. It also offers a reduction of the amount cables.

Some concerns about TFP-SVD are the feasibility and efficiency of the final sensor production and the small signal charge due to the short path length of the particles through the sensor.

In any case a first prototype has been produced by Micron-Semiconductor Ltd (UK), with a size of $52.6 \times 59.0 \text{ mm}^2$. The characterization studies are in agreement with the expectation and also a lower full depletion voltage is confirmed (??). It is planned to increase the dimensions to $100 \times 100 \text{ mm}^2$ in the further prototype.

2.3.3 Silicon On Insulator (SOI)

The basic idea of the proposal is to replace the whole VXD detector employing a new design of pixel, called Dual Timer Pixel (DuTiP), based on SOI technology. This new sensor concept has been invented to cope with the expected higher background accordingly to higher value of luminosity to achieve.

2.3.3.1 Concept

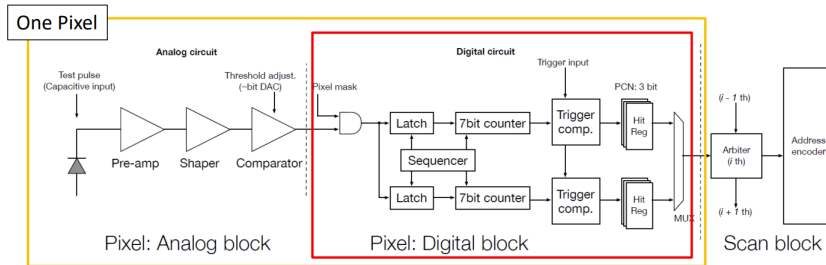
SOI technology has been chosen as baseline for the new pixel design thanks to its monolithic structure, thinness, low power consumption and low parasitic capacitance. In addition it's resistant against neutron and single event upset (SEU, explained??), even though an important issue is TID effect on which efficient solutions have been studied.?

To cope with higher background environment indeed, DuTiP was invented to fulfill the requirements of a new vertex detector with faster readout, lower

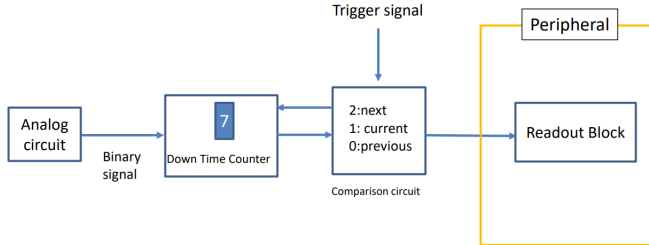
occupancy, smaller data size and smaller data transfer. In particular its concept rest on the concern to store at least two hits during Belle II trigger latency of $4.5 \mu\text{m}$, to avoid loss information of the inner part of the detector at high background level.

The analog part is quite standard for a binary detector and consists of a sequence of preamplifier, shaper and comparator. Digital part is equipped with two timers (7 bit counters) to store at least two hits. When a processed hit signal arrive to the digital part it is stored and one of the timers start to counting down from a starting time set to trigger latency plus one clock, waiting for trigger signal. If the trigger signal is received when the time is 1 (it could be also 2/0), the signal is readout as current (Next/Previous respectively) timing (PreviousCurrentNext, PCN timings?). If the trigger is not received at the PCN timings in the pixel, the timer is reset.

This complicated digital circuit has to be assembled on each pixel and Lapis semiconductor $2.0 \mu\text{m}$ FD-SOI CMOS technology has been chosen, based on the experience gained in the successful development of other detectors like pixel detectors for the future ILC and CEPC.?



(a) Analog, Digital and Scan blocks for DuTiP detector.



(b) Operational sketch.

Figure 2.1: Schematic of DuTiP circuits.

2.3.3.2 Sensor design and features

The size fo the new designed pixel is $45 \mu\text{m}$ and the sensor layer thickness of $50 \mu\text{m}$, which gives about $11 \mu\text{m}$ of intrinsic resolution on z direction averaging over incident polar angle. ALPIDE was choosen as analog circuit with some modification to adapt it to SOI technology.

DuTiP pixel detector is designed to cover the current VXD acceptance with 7 layer: 1-3 with S (smaller size chip) type sensors, 4-7 with L(larger size) type

instead (on this page).

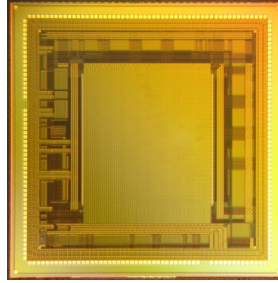
sensor type	layer	pitch [μm]	row \times column [pixels]	array $r\phi \times z$ [mm^2]	array area [cm^2]	chip $r\phi \times z$ [mm^2]
S	1–3	45	320 \times 640	14.4 \times 28.8	4.15	17.2 \times 29.6
L	4–7	45	480 \times 640	21.6 \times 28.8	6.22	24.4 \times 29.6

Figure 2.2: The size of Small (S) and Large (L) DuTiP chips.

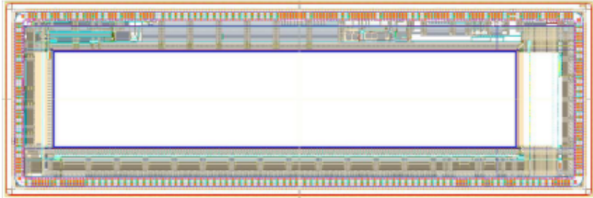
In order to minimize the dead region between chips in the ladder, stitching technique allows to produce longer chips in the z direction, but the structure of the ladders has not be decided yet. For the inner layer of the detector might be possible the cooling with airflow at room temperature; for the outer layers instead, a combination of air and water flows.

For layer 1, which is expected to work in more severe condition of background, the pixel occupancy has been estimated with the trigger latency of 8.0 μs and both (L and S?) are small enough, $O(10^{14})$ or less, thus stabøe tracking and vertexing are contemplated. Moreover without using two timers for layer 1, the signal loss probability with the trigger latency of 4.5 (8.0) μs is about 0.2 (0.4)% and so not negligible. In fact if the background rate is higher and the latency is longer, the signal loss probability increases.

A first prototype of this new desgin has been delivered in June 2021, with all in-pixel functionalites except for the scan block and the fast readout system. the chip is a matrix of 64x64 pixels and size of 6x6 mm^2 . Its characterization is ongoing and it seems to work fine, aslo with radioactive sources and red laser. A second prototype had been submitted in December 2021, with 64x320 pixels and size of 18x6 mm^2 (on the current page).



(a) DuTip first prototype.



(b) DuTip second prototype.

Figure 2.3: DuTiP prototypes.

2.3.4 CMOS MAPS

The last proposal is the one that we will analyze in more details in the next chapters. Like the previous one, it aims to replace the entire current VXD detector using a new technology, in this case the CMOS MAPS, that is Monolithic Active Pixel Sensor CMOS (Complementary Metal-Oxide Semiconductor).

The program hopes to solve some of the issues discussed in the previous chapters, with a new system of two inner layers and three outermost, for a total of 5 stages equipped with a single sensor type, called **VTX** (on this page). Also the mechanical structure had been redesigned but it is expected that the all system could work at room temperature, so as consequence an important reduction of services is also contemplated.

The new pixel design is called OBELIX, based on the pixel matrix of the TJ-Monopix 2 chip, whose characterization is the main topic of this work.

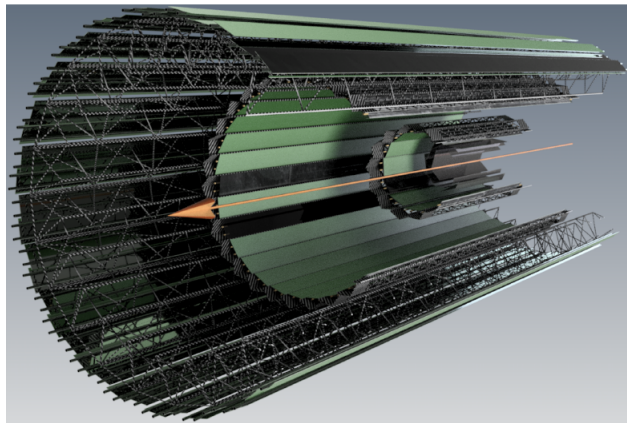


Figure 2.4: Overall VTX layout.

At the current state of art, intense R&D(Research and Development) is being carried out, taking advantage from other experiments experiences, like ALICE, with the same type of sensor.

After a briefly review of the main upgrade proposals, we can now deepen into this last one in the following chapter.

3. VTX detector

This chapter focuses on one of the four proposal for the vertex detector upgrade of Belle II, that is VTX. After a brief reference to the reasons behind the vertex detector upgrade, we will go through VTX concept and layout, designed with a new geometry with respect VXD and so with a different mechanical structure and a new pixel sensor, in order to fulfill the new requirements dictated by new environment conditions. Moreover all ongoing studies are supported by continual tests and simulations that we will also take a look at.

3.1 VTX Layout and mechanical structure?

In section on page 10 we have introduced in a few word the concept of the *nano-beam* scheme, which could allow to achieve the new fixed target of instantaneous luminosity. This new strategy required a strong focusing of the beams in particular at the IP, resulting in a large amounts of beam induced background and as consequence in a higher dose of radiation in the innermost detector layers, which therefore have to be robust enough to keep good performance. Furthermore, to be able to reach the target luminosity, SuperKEKB might have to consider an improvements of the final focusing magnets and so a potentially re-design of the interaction region, including the detector (regardless of the hit rates and radiation hardness issue?).

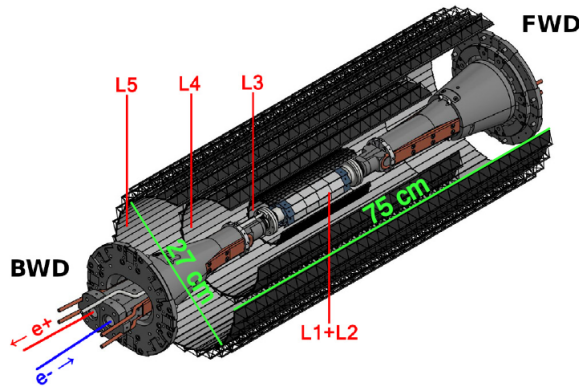


Figure 3.1: Concept of VTX layout with 5 barrel layers, filling the current VXD volume.

So VTX aims to replace the all VXD with a fully pixelated detector based on Depleted Monolithic Active Pixel Sensors (DMPAS) arranged on five layers at different distance from the beam pipe. Actually the radii and the number of the layers are currently subject to studies and simulations in order to achieve an optimized arrangement(?) (figure on the facing page). As already discussed for other upgrade proposal, it may be important to try to reduce the material budget, in order to minimize the multiple Coulomb scattering which particularly affects the very soft particles produced in Belle II collisions. By using a single sensor type, it is expected a reduction of the overall material budget up to 2% of radiation lenght, against the present 3% of VXD, which uses two different sensors such as pixels and strips.

3.1.1 iVTX

The *internal*VTX consists of the first two detector layers devised together with a self-supported air-cooled all-silicon ladder concept, where four contiguous sensors are diced out of a wafer, thinned and interconnected with post-processed redistribution layers. They are designed to be at 1.4 and 2.2 cm respectively from the beam pipe, and to target an individual material budget of about 0.1% radiation lenght. This is actually achievable because the overall surface of this layers is moderate, below 400 cm^2 , the low sensor power dissipation and the few connections needed for the operation.

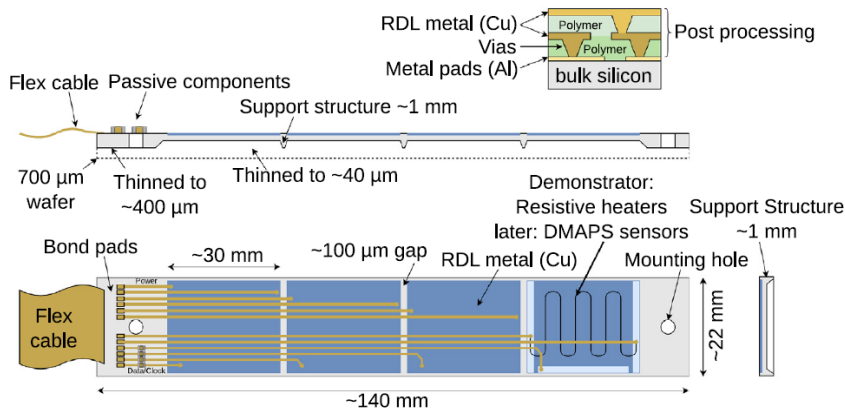


Figure 3.2: Sketch of the all-silicon ladder concept of the iVTX. Four dummy sensors are shown in blue on the silicon support in grey. The yellowish lines instead, indicate power and data transmission lines. Power is delivered to the ladder by a flex cable, which also transmits data to and from the chips in the final chips.

In figure on the current page is showing a sketch of the iVTX demonstrator ladder, 140 mm long and 22 mm wide (grey). Instead of the actual sensors, it is equipped with four dummies chips with a lenght of about 30 mm (blue), which are used as resistor to mimic the estimated heat load in order to test the air cooling system. A redistribution layers (RDL) for power and data is also added to the demonstrator, to connect the chips with a flex cable at the end of the ladder (yellowish lines). In addition the wafer is thinned to 400 μm and the

sensitive areas down to $40 \mu\text{m}$, to test the mechanical integrity.

3.1.1.1 R&D

The R&D is ongoing. First thinned ladders have been produced and characterised with different thickness and geometry, revealing a homogeneous thickness over an area of 10 cm^2 .

In addition tests are focused on evaluating power delivery efficiency, the quality of the signal which travel through the ladder and also the process used to fully assemble it. In figure on this page are shown eye diagrams from simulation with a transfer rate of 640 Mbps, which may imply that 320 Mbps of data rate will be possible. (??)

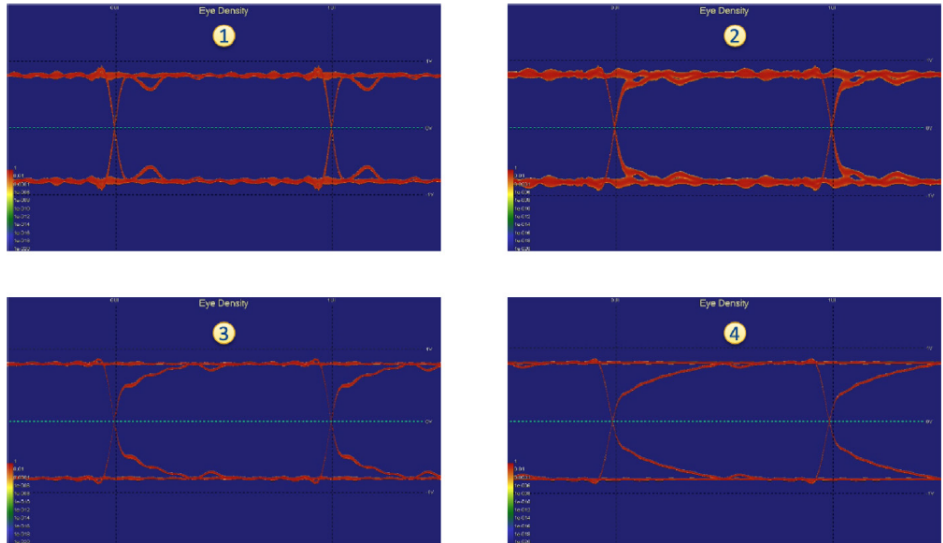


Figure 3.3: Eye diagrams of the iVTX data transmission lines at four different locations on the ladder.

3.1.2 oVTX

The *outer?*VTX consists of three layers respectively at radii of 3.9, 9 and 14 cm from the beam pipe and because of the larger distance required to cover the acceptance, they are not self-support. They follow a more traditional approach, strongly inspired by the designed developed for the ALICE ITS2. Each ladder is water cooled and made of a light carbon fiber support structure, called *truss*, which provide the mechanical integrity. Its structural design is showed in figure on the next page: 70 cm long and 5.8 g of weight, it is able to support more than 40 sensors in two rows next to each other with a small overlap, earning a material budget of $0.3\% X_0$ for the first two layer and $0.8\% X_0$ for the outermost one.

For the cooling of the ladder, it is developing a cold-plate concept (figure on page ??), on which the sensors are glued and that in turn is installed on the truss. For each row, there is a polyimide cooling tube that runs over all the

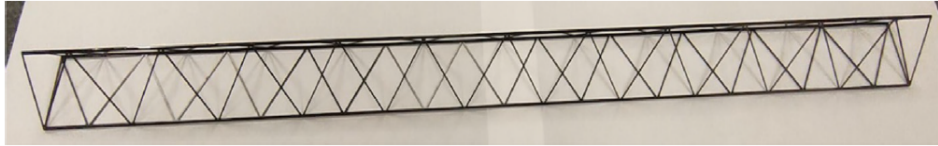


Figure 3.4: Prototype of the layer 5 *truss*, which is the longest, made from thin carbon fibre structures.

sensors and turns back at the other end, so that the heated coolant leaves on the same side.



Figure 3.5: A prototype of the cold-plate for colling. One coolant tube(golden) is connected to the cold plate(black) and turns 180° on the other end (not shown) so that the coolant flows in both directions and thus leaves on the same side it starts.

In figure on the current page is shown the several structures described that shape a ladder of the outermost layer 5. From bottom to top come in succession the carbon fibre structure, two cold-plates for the two neighbouring sensor rows (Chips, in grey) and the flex cables for power and data transmission (green).

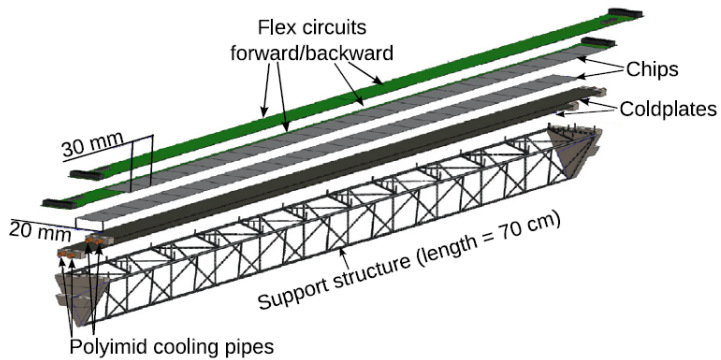


Figure 3.6: An exploding drawing of a fully assembled layer 5 ladder.

3.1.2.1 R&D

After the assembly described in the previous, first thermo-mechanical tests were performed and they show that the first resonance frequency is at 200 Hz, which is above the one of the typical earthquakes in Japan and also that the thermal

properties are good.

Trying to reduce as much as possible the material budget, the transmission lines and the flex cables has to be as thin as possible, but also need to ensure safe data transmission. For this reason, the outermost ladders long 70 cm are equipped with two flex cables, one from each side of the *truss*. In figure on this page the resulting eye diagram from testing the signal integrity of one of the 35 cm long transmission lines for data transmission rate of 500 Mbps. A clear difference between high and low indicates a good starting point for further developments.

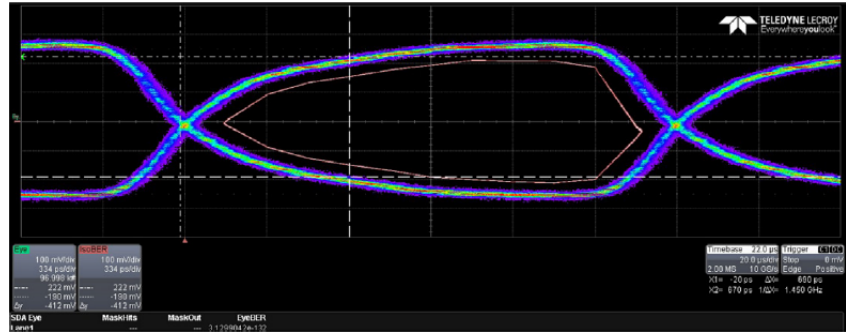


Figure 3.7: Eye diagram for the oVTX transmission line signal integrity of the layer 5 flex cable.

3.2 Performance simulation

3.3 OBELIX chip design

As we already seen, the VTX detector is designed with a single type sensor taylored to the specific need of Belle II, called OBELIX (Optimized BELle II pIXel sensor) and currently under development, based on fast and high granular Depleted Monolithic Active Pixel Sensor (DMAPS). This new designed sensor comes from an evolution of TJ-Monopix 2, whose characterization is the main topic of this thesis, and which will be discussed in (reference) and both of them relies on the CIS? 180 μ m process by TowerJazz Semiconductor. As a matter of fact its predecessor is equipped with four different flavors (reference), and for now the final decision on which to use for Obelix has not been made.

A schematic layout of the chip is shown in figure on the next page. The size of the sensor is expected to be 3 x 2 cm^2 , with an active area of 3 x 1.5 cm^2 and an additional part in the periphery of about 3 x 0.3 cm^2 dedicated to data pre-processing and triggering. The pixel pitches are designed to be from 30 μ m to 40 μ m in both direction. To deal with the target hit rate of 120 MHz/ cm^2 , the timestamp clock signal can reach down to 25 ns, even if studies have demonstrated that a window of 100 ns is enough to limit to 320 Mbps the data throughput at the same expected hit rate. With respect to TJ-Monopix 2,

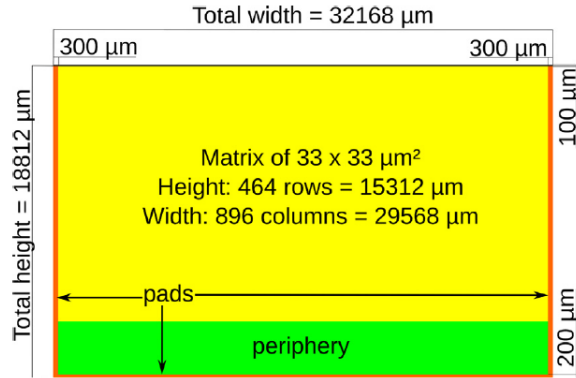


Figure 3.8: OBELIX chip design.

which is equipped with a triggerless column-drain readout without memory at the periphery, OBELIX must have a triggered readout architecture, in order to satisfy the needs of Belle II. Moreover the latency is fixed to $5 \mu\text{s}$ and it might operate up to 30 KHz trigger rate. The expected power consumption instead, is expected to be about 200 mW/cm^2 .

Its main design features are summarised in on this page.

Pixel pitch	30 to 40 μm
Matrix size	512 rows \times 928 to 752 columns
Time stamping	25 to 100 ns precision over 7 bits
Signal Time over threshold	7 bits
Output bandwidth	320 to 640 Mbps
Power dissipation	100 to 200 mW/cm 2
Radiation tolerance	100 MRad and $10^{14} \text{ n}_{\text{eq}}/\text{cm}^2$

Figure 3.9: Designed features of the OBELIX sensor.

4. Conclusions

List of Figures

1.1	Particle classification in the Standard Model.	4
1.2	Example of the kinematics of the golden channel of Belle II experiment.	8
1.3	SuperKEKB accelerator structure.	9
1.4	Beam energies to reach center of mass energy equal to $\Upsilon(4S)$, $\Upsilon(6S)$, 11.24 GeV and 12 GeV. Horizontal axis represents the energy of LER and the vertical one the energy of HER.	10
1.5	Comparison between the beams scheme used in KEKB and SuperKEKB.	11
1.6	Belle II detector.	11
1.7	A schematic view of the Belle II vertex detector with a Be beam pipe and the six layers of PXD and SVD.	12
1.8	TOP detector.	13
1.9	ARICH detector.	13
2.1	Schematic of DuTiP circuits.	21
2.2	The size of Small (S) and Large (L) DuTiP chips.	22
2.3	DuTiP prototypes.	22
2.4	Overall VTX layout.	23
3.1	Concept of VTX layout with 5 barrel layers, filling the current VXD volume.	24
3.2	Sketch of the all-silicon ladder concept of the iVTX. Four dummy sensors are shown in blue on the silicon support in grey. The yellowish lines instead, indicate power and data transmission lines. Power is delivered to the ladder by a flex cable, which also transmits data to and from the chips in the final chips.	25
3.3	Eye diagrams of the iVTX data transmission lines at four different locations on the ladder.	26
3.4	Prototype of the layer 5 <i>truss</i> , which is the longest, made from thin carbon fibre structures.	27
3.5	A prototype of the cold-plate for colling. One coolant tube(golden) is connected to the cold plate(black) and turns 180° on the other end (not shown) so that the coolant flows in both directions and thus leaves on the same side it starts.	27
3.6	An exploding drawing of a fully assembled layer 5 ladder.	27
3.7	Eye diagram for the oVTX transmission line signal integrity of the layer 5 flex cable.	28

3.8	OBELIX chip design.	29
3.9	Designed features of the OBELIX sensor.	29

List of Tables